Contribution from the Department of Chemistry,
Northern Illinois University, DeKalb, Illinois 60115

Electronic and MCD Spectra of Linear Two-Coordinate Dihalo-, Halo(trialkylphosphine)-, and Bis(triethylphosphine)gold(I) Complexes

M. Meral Savas and W. Roy Mason*

Received June 9, 1986

Electronic absorption and magnetic circular dichroism (MCD) spectra are reported at room temperature for acetonitrile solutions of tetra-*n*-butylammonium salts of AuX_2^-, X = Cl^-, Br^-, and I^-, the hexafluorophosphate salt of $Au(PEt_3)_2^+$, and the mixed complexes $AuCl(PR_3)$, R = Me and Et, and $AuX(PEt_3)$, X = Br^- and I^-. The $Au(PEt_3)_2^+$ ion exhibits several strong bands in the UV region, which are assigned as metal to ligand charge-transfer (MLCT) transitions. The AuX_2^- ions show weak low-energy vibronic d → s transitions and higher energy intense d → p transitions. In addition $AuBr_2^-$ and AuI_2^- spectra display ligand to metal charge-transfer (LMCT) transitions. The spectra of the $AuX(PR_3)$ complexes are interpreted as a combination of MLCT, LMCT, and d → p type transitions; the weak d → s transitions are not visible in the spectra of the mixed complexes. Spectral assignments are discussed together with the ligand dependence of relative orbital energies among the highest energy occupied and lowest energy empty MO's.

Introduction

The monomeric complexes of gold(I) ($5d^{10}$ electron configuration) provide some of the best examples of simple linear two-coordination, offering a variety of stable complexes that resists ligand addition and increased coordination.[1] As such, the electronic spectra for representative Au(I) complexes continue to be of interest since they can provide an important experimental basis for electronic structure models of d^{10} two-coordinate complexes. The nature of the molecular orbitals of two-coordinate Au(I) complexes and their low-energy excited states is ligand-dependent, and the nature of this ligand dependence has been the motivation for a systematic investigation of typical Au(I) complexes in this laboratory in recent years.[2-4] For example, the lowest energy excited states for $AuCl_2^-$ and $AuBr_2^-$ were interpreted from spectral data as resulting from metal-localized 5d → 6s and 5d → 6p transitions, while those of AuI_2^- include also states of the ligand to metal charge-transfer (LMCT) type.[3] In contrast the lowest energy states for Au(I) complexes with π-cceptor ligands (CN^-, CNR, $P(OR)_3$) have been assigned as metal to ligand charge-transfer (MLCT) states.[2,4] The ligand dependence of the lowest energy excited states implies changes in the nature of the highest occupied molecular orbitals (HOMO's) and lowest unoccupied molecular orbitals (LUMO's) in these Au(I) complexes. Relative orbital participation in bonding is thus sensitive to the ligand. This same conclusion has also been reached by some recent SCF-MS-Xα calculations on AuX_2^-, X = Cl^-, Br^-, I^-, and CN^-.[5]

In this paper we report some new electronic absorption and magnetic circular dichroism (MCD) spectral measurements in acetonitrile solution for tetra-*n*-butylammonium (TBA) salts of AuX_2^-, X = Cl^-, Br^-, and I^-, the hexafluorophosphate salt of $Au(PEt_3)_2^+$, and the mixed complexes $AuCl(PR_3)$, R = Me and Et, and $AuX(PEt_3)$, X = Br^- and I^-. Some low-field (1 T) MCD spectra were reported earlier from our laboratory[3] for the AuX_2^- ions, but the new spectra described herein were obtained at higher field (7 T) and with greatly improved signal to noise. The new spectra reveal several new features, especially in the region of the weak low-energy bands assigned as 5d → 6s transitions. MCD spectra for the $AuX(PR_3)$ and $Au(PEt_3)_2^+$ complexes have not been reported before.

Experimental Section

The chloro(trialkylphosphine)gold(I) complexes, $AuCl(PMe_3)$ and $AuCl(PEt_3)$, were purchased (Johnson-Matthey/AESAR) and were subjected to elemental analysis and characterized by ^1H and ^{31}P NMR[6] before they were used. Tetra-*n*-butylammonium (TBA) salts of AuX_2^-, X = Cl^-, Br^-, and I^-, were prepared as described earlier.[3,7] Bromo(triethylphosphine)gold(I) was prepared by treating a solution of $(TBA)[AuBr_2]$ in tetrahydrofuran with triethylphosphine. The white crystalline $AuBr(PEt_3)$ precipitated when 2:1 H_2O/ethanol was added to the THF solution. Iodo(triethylphosphine)gold(I) was prepared by treating $AuCl(PEt_3)$ with (TBA)I in ethanol solution. The white $AuI(PEt_3)$ precipitated upon addition of water to the ethanol solution. The complex $AuCl(PEt_3)$ also served as the starting material for $[Au(PEt_3)_2]PF_6$; both PEt_3 and Et_4NPF_6 were added to an acetone solution containing the starting material. Evaporation of this solution under reduced pressure gave an oily substance that was washed thoroughly with water to remove Et_4NCl and then stirred with ether, which promoted formation of soft white crystals. All of the compounds gave satisfactory elemental analyses.

Electronic absorption spectra were determined by using a Cary Model 1501 spectrophotometer, while MCD and absorption spectra were determined simultaneously and synchronously along the same light path by using a computer-controlled spectrometer built in our laboratory.[8] Magnetic fields of 7 T were provided by a superconducting magnet system (Oxford Instruments SM2-7, fitted with a room-temperature bore tube). Spectral grade acetonitrile was used throughout, and all spectra were corrected by subtracting the solvent blank. The solutions of the gold complexes showed no changes over the times required for the spectral measurements, and Beer's law was found to hold within experimental error in each case.

Experimental MCD $\bar{A}_1$ and $\bar{B}_0$ parameters were determined by the method of moments.[9] The average energy about which the moments were determined, $\bar{\nu}_0$, was obtained by setting the first moment of the absorption to zero. $\bar{A}_1$ parameters were found from $\int(\Delta\epsilon_M/\bar{\nu})(\bar{\nu}-\bar{\nu}_0)\,d\bar{\nu} = \langle\Delta\epsilon_M\rangle_1 = 152.5\bar{A}_1$, $\bar{B}_0$ parameters from $\int(\Delta\epsilon_M/\bar{\nu})\,d\bar{\nu} = \langle\Delta\epsilon_M\rangle_0 = 152.5\bar{B}_0$, and values of $\bar{D}_0$ (the dipole strength) from $\int(\epsilon/\bar{\nu})\,d\bar{\nu} = \langle\epsilon\rangle_0 = 326.6\bar{D}_0$. The quantity $\Delta\epsilon_M$ is the differential molar absorptivity per unit magnetic field with units of M^{-1} cm^{-1} T^{-1}.

Results and Discussion

Figures 1-4 present electronic absorption and MCD spectra for acetonitrile solutions of $(TBA)[AuCl_2]$, $AuCl(PEt_3)$, $AuI(PEt_3)$, and $[Au(PEt_3)_2](PF_6)$, respectively; spectra for $(TBA)[AuBr_2]$, $(TBA)[AuI_2]$, $AuCl(PMe_3)$, and $AuBr(PEt_3)$ were of comparable quality. Table I summarizes quantitative spectral data for all the complexes investigated. The MCD spectra for the AuX_2^- ions measured here at 7-T field are of considerably higher quality than our earlier low-field results[3] and in addition include the weak low-energy bands for AuI_2^- (bands I and II), which could not be studied before because of the weakness of the MCD signals. In the higher energy region for each of the AuX_2^- ions, where the MCD signals are stronger, the present results agree

(1) Puddephatt, R. J. *The Chemistry of Gold*; Elsevier: Amsterdam, The Netherlands, 1980.
(2) Mason, W. R. *J. Am. Chem. Soc.* **1976**, *98*, 5182.
(3) Koutek, M. E.; Mason, W. R. *Inorg. Chem.* **1980**, *19*, 648.
(4) Chastain, S. K.; Mason, W. R. *Inorg. Chem.* **1982**, *21*, 3717.
(5) Bowmaker, G. A.; Boyd, P. D.; Sorrenson, R. J. *J. Chem. Soc., Faraday Trans. 2* **1985**, *81*, 1627.
(6) Mays, M. J.; Vergnano, P. A. *J. Chem. Soc., Dalton Trans.* **1979**, 1112.
(7) Braunstein, P.; Clark, R. J. H. *J. Chem. Soc., Dalton Trans.* **1973**, 1845.
(8) Mason, W. R. *Anal. Chem.* **1982**, *54*, 646.
(9) Piepho, S. B.; Schatz, P. N. *Group Theory in Spectroscopy with Applications to Magnetic Circular Dichroism*; Wiley-Interscience: New York, 1983. This reference describes the standard (Stephens) definitions and conventions which are used here throughout.

0020-1669/87/1326-0301$01.50/0

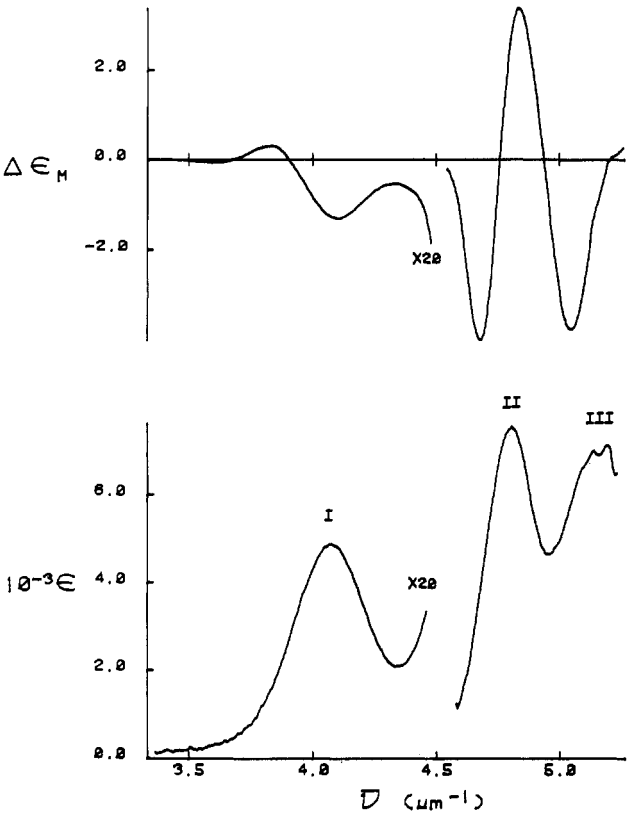

Figure 1. Absorption (lower curves) and MCD (upper curves) spectra for (TBA)[$AuCl_2$] in acetonitrile. Both left-hand curves were multiplied by a factor of 20 before plotting.

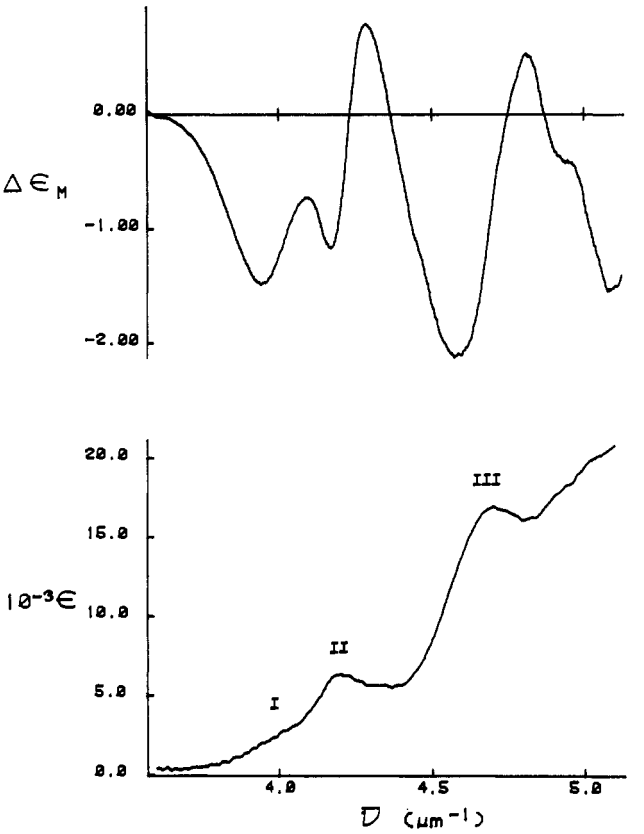

Figure 3. Absorption (lower curve) and MCD (upper curve) spectra for AuI(PEt_3).

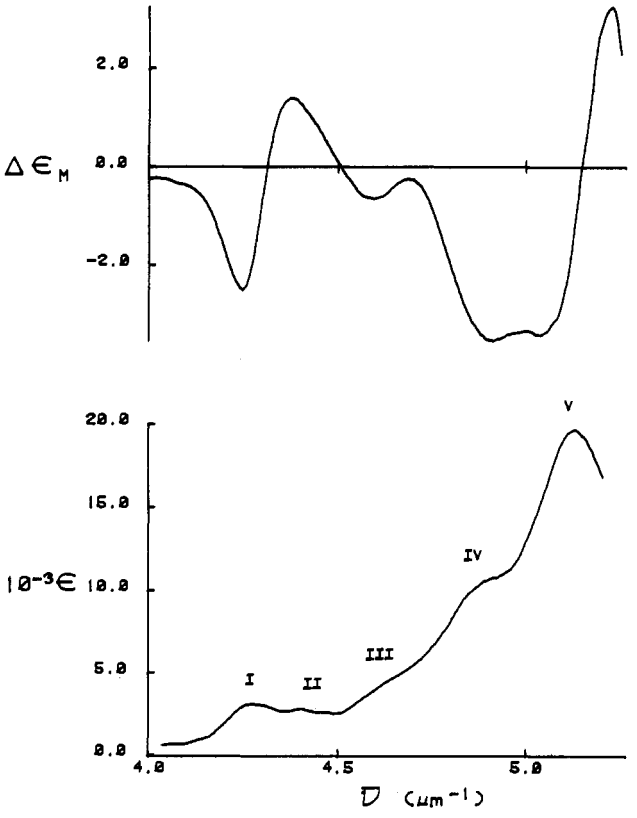

Figure 2. Absorption (lower curve) and MCD (upper curve) spectra for AuCl(PEt_3) in acetonitrile.

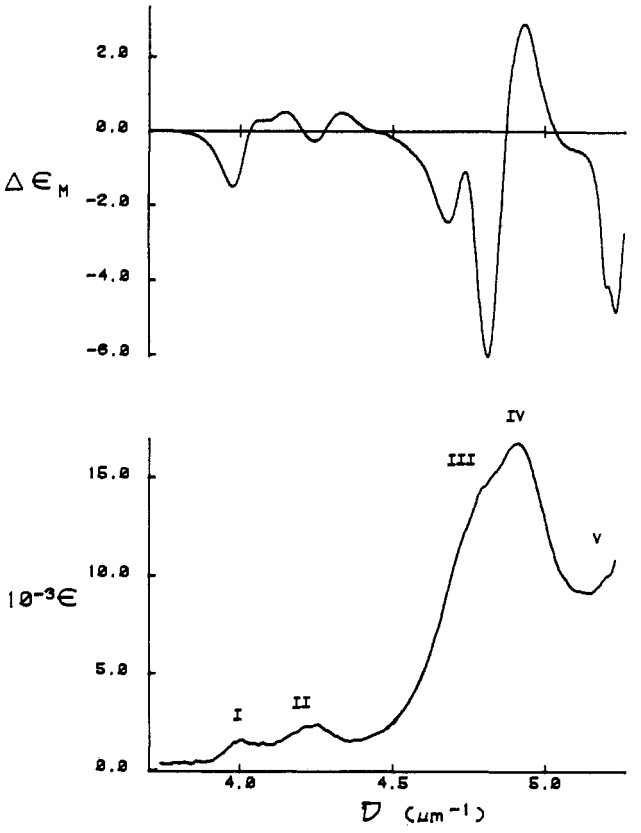

Figure 4. Absorption (lower curve) and MCD (upper curve) spectra for [$Au(PEt_3)_2$](PF_6) in acetonitrile.

favorably with the peak positions and relative intensities reported earlier. The lowest energy bands for the AuX_2^- ions (bands I and II for $AuCl_2^-$, band I for $AuBr_2^-$ and AuI_2^-) exhibit MCD *A* terms and absorption maxima that are separated from adjacent bands sufficiently so that a moment analysis of the spectra was deemed feasible. The results are collected in Table II. The analysis is sensitive to the energy range taken from the low-energy side of the band to the high-energy side, and overlapping bands on either

Table I. Spectral Data for Acetonitrile Solution

band	absorption			MCD		band	absorption			MCD	
no.	$\bar{\nu}$, μm^{-1}	λ, nm	ϵ, M^{-1} cm^{-1}	$\bar{\nu}$, μm^{-1}	$\Delta\epsilon_M$, M^{-1} cm^{-1} T^{-1}	no.	$\bar{\nu}$, μm^{-1}	λ, nm	ϵ, M^{-1} cm^{-1}	$\bar{\nu}$, μm^{-1}	$\Delta\epsilon_M$, M^{-1} cm^{-1} T^{-1}
					(TBA)[$AuCl_2$]						
				3.59	-2.98×10^{-3}					4.68	−3.97
				3.83	$+1.52 \times 10^{-2}$					4.76	0
I	4.05	247	244	3.90	0	II	4.78	209	7520	4.84	+3.37
				4.10	-6.54×10^{-2}					5.05	−3.75
						III	5.14	194	7030[a]	5.19	0
										[c]	
					(TBA)[$AuBr_2$]						
				3.39	-1.30×10^{-3}					4.63	−4.22
				3.63	$+1.75 \times 10^{-2}$	III	4.71	212	10700	4.72	0
I	3.90	257	169	3.73	0					4.75	+0.91
				3.93	-6.33×10^{-2}	IV	4.99	201	12600	4.94	−2.94
II	4.50	222	3600[a]	4.42	−1.04[a]	V	5.16	194	12700	5.18	−0.46
					(TBA)[AuI_2]						
				2.42	-2.45×10^{-3}					4.18	−2.89
I	2.77	362	101	2.62	0	IV	4.32	231	9900[a]	4.29	0
				2.77	$+2.73 \times 10^{-3}$					4.38	+1.86
II	3.46	289	290	3.31	-1.64×10^{-2}	V	4.59	218	20300	4.56	−1.77
III	4.03	248	4000[a]	4.01	−2.85					4.75	−2.75
						VI	4.92	203	26500[a]	4.96	−8.06
					$AuCl(PMe_3)$						
I	4.28	234	2030	4.26	−2.10					5.04	−3.50
II	4.42	226	1940	4.39	+1.06	IV	5.16	194	17600	5.18	0
				4.67	−0.97					5.24	+2.09
III	4.90	204	8700[a]	4.95	−3.29[a]						
					$AuCl(PEt_3)$						
I	4.25	235	2010	4.26	−2.47					5.04	−3.38
II	4.37	229	1720[a]	4.37	+1.40	V	5.11	196	15000	5.14	0
III	4.65	215	3250[a]	4.59	−0.63					5.22	+3.23
IV	4.90	204	7300[a]	4.90	−3.52						
					$AuBr(PEt_3)$						
I	4.24	236	2700[a]	4.22	−2.73					4.85	−5.55
				4.34	+0.43	III	5.01	199	16500	5.01	0
II	4.46	224	3800[a]	4.43	−0.21					5.10	+4.62
				4.55	+1.36						
					$AuI(PEt_3)$						
I	3.95	253	1320[a]	3.94	−1.48					4.58	−2.10
				4.17	−1.17	III	4.69	213	16000	4.75	0
II	4.20	238	5100	4.23	0					4.81	+0.53
				4.28	+0.79					4.94	−0.41[a]
										5.08	−1.52
					$[Au(PEt_3)_2](PF_6)$						
I	3.98	251	1150	3.97	−1.49	III	4.78	209	14000[a]		
				4.06	+0.31					4.81	−6.04
II	4.20	238	1740	4.16	+0.52	IV	4.88	205	15500	4.87	0
				4.24	−0.26					4.93	+2.90
				4.33	+0.50	V	5.08	197	14200[a]	5.09	−0.48[a]
				4.68	−2.45					5.20	−4.17[a]
						VI	5.22	192	12000[a]	5.23	−4.84

[a] Shoulder. [b] *A* term. [c] Insufficient data.

Table II. Spectral Band Properties for AuX_2^-

band no.	$\bar{\nu}_{max}$, μm^{-1}	$\bar{\nu}_{1/2}$,[a] μm^{-1}	ϵ, M^{-1} cm^{-1}	moment anal.[b] $\bar{\nu}_0$, μm^{-1}	$\bar{A}_1/\bar{D}_0$	$10^4\bar{B}_0/\bar{D}_0$, cm	$\bar{D}_0$, D
			(TBA)[$AuCl_2$]				
I	4.05	0.38	244	4.03	−0.6 ± 0.1	−3 ± 1	3.8×10^2
II	4.78	0.28	7520	4.76	+1.8 ± 0.2	−2.1 ± 0.3	0.528
			(TBA)[$AuBr_2$]				
I	3.90	~0.39	169	3.84	−1.9 ± 0.05	−4 ± 1	1.5×10^{-2}
			(TBA)[AuI_2]				
I	2.77	0.47	101	2.72	+0.1 ± 0.02	+1.4 ± 0.5	1.7×10^{-2}

[a] Width at half-height. [b] Error limits estimated from repetitive determinations using different energy ranges about the absorption maximum.

side can affect the results. In some cases the error limits on $\bar{A}_1/\bar{D}_0$ and $\bar{B}_0/\bar{D}_0$ (Table II) are larger than desirable due to the overlap. However, in the worst cases the sign and approximate magnitude are probably reliable to within the limits indicated.

Molecular Orbitals, Excited States, and MCD Terms. Figure 5 shows schematic MO energy level diagrams for the $D_{\infty h}$ AuX_2^-

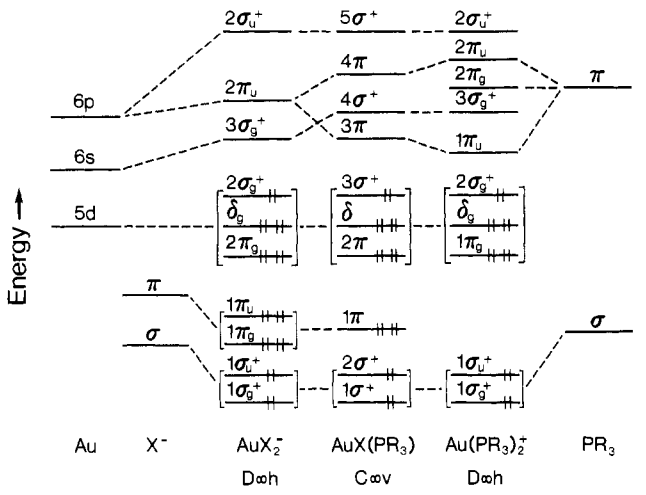

Figure 5. One-electron MO energy levels.

and $Au(PEt_3)_2^+$ ions and the $C_{\infty v}$ $AuX(PR_3)$ complexes that will be suitable for a discussion of the electronic spectra. In each case the z axis is taken along the molecular axis. The ground-state electron configuration for each type of complex is shown in the diagrams. These configurations consist of all paired electrons, and therefore the ground state of each complex is diamagnetic, nondegenerate and designated $^1\Sigma_g^+$ or $^1\Sigma^+$. Electric-dipole-allowed transitions are restricted to transitions to Σ_u^+ or Σ^+ (z polarized) and Π_u or Π (x,y polarized) excited states of $D_{\infty h}$ or $C_{\infty v}$, respectively. It should be recognized, however, that because spin–orbit interaction is large for orbitals involving the heavy atoms Au, I, and Br, singlet and triplet spin designations of excited states will lose their significance. States of both singlet and triplet origin in the absence of spin–orbit coupling will become intermixed in spin–orbit states, the consequence of which will allow transitions to states of formally triplet parentage to gain appreciable intensity.

The degenerate Π_u or Π excited states can give rise to MCD A terms as a result of Zeeman splitting by the longitudinal magnetic field.[9] The sign and magnitude of the A terms for transitions to the states j = Π_u or Π in solution can be expressed in terms of the space-averaged parameter ratio $\bar{A}_1/\bar{D}_0$. This ratio can be calculated from eq 1,[9] where $\bar{D}_0 = -^1/_3|\langle a||\mathbf{m}^{\Pi}||j\rangle|^2$, the

$$\bar{A}_1/\bar{D}_0 = -(1/2^{1/2}\mu_B)\langle j||\mu^{\Sigma^-}||j\rangle \qquad (1)$$

dipole strength of the transition a → j (a = Σ_g^+ or Σ^+, the nondegenerate ground state, and $\mathbf{m} = e\mathbf{r}$, the electric moment operator), μ_B = Bohr magneton, and $\mu = -\mu_B(\mathbf{L} + 2\mathbf{S})$, the magnetic moment operator. Both Π_u or Π and Σ_u^+ or Σ^+ excited states can also exhibit MCD B terms, which result from mixing of states by the field. B terms are given by the $\bar{B}_0$ parameter (eq 2),[9] where

$$\bar{B}_0(a \rightarrow p) = \mathrm{Re}\left(-2/(3(2^{1/2})\mu_B)\sum_{q\neq p}\frac{\langle p||\mu^{\Sigma^-}||q\rangle}{W_q - W_p}\langle a||\mathbf{m}^{\Pi}||p\rangle\langle q||\mathbf{m}^{\Pi}||a\rangle\right) \qquad (2)$$

p = Π_u or Π, Σ_u^+ or Σ, q ≠ p = Π_u or Π, W_q and W_p = energies of states q and p, respectively, and the other symbols have the same meaning as in eq 1. B terms are more difficult to calculate because of the summation over all states in eq 2. Estimates can sometimes be made if the states that interact are close in energy and the summation can be limited to only a few terms. This was possible in our previous study of $Au(CN\text{-}Et)_2^+$.[4] Finally it may be remarked that MCD C terms will be zero because the ground states are nondegenerate and diamagnetic.

The first task in interpretation of electronic spectra is to identify the excited configurations responsible for the lowest energy excited states for each complex. As noted above, our previous interpretation for the AuX_2^- spectra identified d → s, d → p, and LMCT transitions.[3] Furthermore, the pattern of the absorption and MCD spectra found here for $Au(PEt_3)_2^+$ (Figure 4) is remarkably similar to spectra for $Au(P(OMe)_3)_2^+$, which was interpreted previously as MLCT.[4] The transitions for the $AuX(PR_3)$ complexes are logically expected to be related to those observed for AuX_2^- and $Au(PEt_3)_2^+$. Therefore, four types of transitions are considered reasonable for the complexes of the present study: (1) d → s, (2) d → p, (3) LMCT, and (4) MLCT. Table III shows the lowest energy excited configurations associated with each transition type, together with the various states that are possible. Included also in Table III are the values of $\bar{A}_1/\bar{D}_0$ calculated from eq 1 for each Π_u or Π state. It may be noted that the d → p and MLCT transitions have exactly the same excited-state symmetries because the symmetries of the MO's involved are the same. In fact, the two types of transitions are closely related because the ligand-based π-acceptor orbitals of the P-donor ligands in the two-coordinate complexes have the same symmetry as the 6p π atomic orbitals of Au. Therefore, the lowest energy virtual orbitals associated with MLCT transitions ($1\pi_u$ or 3π in Figure 5) will be composed of *both* Au 6p and P-donor π contributions to varying degrees. Consequently, the distinction between d → p and MLCT may be void of significance in Au(I) complexes with π-acceptor ligands.

AuX_2^- Spectra. The AuX_2^- spectra can be divided into two regions based on intensity: a low-energy region in which one or more weak ($\epsilon < 300$ M^{-1} cm^{-1}) bands are found and a higher energy region where the absorption is more intense ($\epsilon > 3000$ M^{-1} cm^{-1}). Earlier studies[3] showed that the low-energy weak bands for $AuCl_2^-$ and $AuBr_2^-$ decreased in absorption intensity on cooling to 26 K. As a consequence these bands were assigned to parity-forbidden vibronic d → s transitions. The MCD for these bands was found to be weak and could not be determined completely. The present MCD measurements reveal more detail with greater reliability. Each complex shows a weak negative feature followed by an unsymmetrical negative A term in the region of band I (see for example Figure 1). The negative A term can be interpreted within the Herzberg–Teller approximation for a d → s transition to a Π_g excited state.[10] This approximation assumes only excited-state mixing and coupling of states of only a single symmetry. The triatomic ions provide a simple straightforward application of the approximation because only two odd-parity vibrations are possible: $\nu_2(\pi_u)$ and $\nu_3(\sigma_u^+)$. The only dipole-allowed possibility for a Π_g state that preserves the transition degeneracy corresponds to a ν_3 enabling vibration and coupling with an allowed Π_u excited state at higher energy.[11] In this approximation a negative A term is predicted. Therefore, the most logical assignment for band I for $AuCl_2^-$ and $AuBr_2^-$ is to the transition to $\Pi_g(^1\Pi_g)[(2\pi_g)^3(3\sigma_g^+)]$. The other possible Π_g states among the d → s configurations (see Table III) are of triplet parentage, and transitions to them would be expected to be weaker. It is interesting that the $\bar{A}_1/\bar{D}_0$ value (Table II) observed for $AuBr_2^-$ (−1.9) is significantly larger than for $AuCl_2^-$ (−0.6). This difference may signal the presence of a weak transition to the $\Pi_g(^3\Sigma_g^+)$ d → s state (see Table III) in the region of band I for $AuBr_2^-$. However, another reasonable possibility for the larger $\bar{A}_1/\bar{D}_0$ value for $AuBr_2^-$ is a vibronic state or states associated with the parity-forbidden excited LMCT configuration $(1\pi_g)^3(3\sigma_g^+)$, which will also give rise to Π_g states. From earlier assignments[3] of the more intense bands of $AuBr_2^-$ (see below), the possibility exists for a low-energy, parity-forbidden LMCT in the energy region of band I, and such a state, especially if of spin-forbidden origin, could contribute significantly to the observed $\bar{A}_1/\bar{D}_0$. The corresponding LMCT state or states for $AuCl_2^-$ would be expected at higher energy than band I so that the $\bar{A}_1/\bar{D}_0$ value would be reflective of the d → s state alone.

The weak negative MCD feature observed to the red of the negative A term for $AuCl_2^-$ and $AuBr_2^-$ is likely due to one or more spin-forbidden vibronic d → s states. No resolved absorption is observed which precludes a term assignment for the MCD, but

(10) Reference 9, Chapter 22.

(11) A reviewer has pointed out that the A term could be two B terms of opposite sign coupling via the pure electronic state with $\nu_2(\pi_u)$. We prefer the simpler interpretation consisting of an A term and a single vibronic Π_g state; however, the present results do not distinguish between the two possibilities.

Table III. Excited Configurations and States

excited config[a]			no spin–orbit coupling[b]	spin–orbit states[b]	calcd $\bar{A}_1/\bar{D}_0$
AuX_2^-	$AuX(PR_3)$	$Au(PEt_3)_2^+$			
		d → s Transitions			
$(2\sigma_g^+)(3\sigma_g^+)$	$(3\sigma^+)(4\sigma^+)$	$(2\sigma_g^+)(3\sigma_g^+)$	$^1\Sigma_g^+$	Σ_g^+	
			$^3\Sigma_g^+$	Σ_g^-	
				Π_g	−2[c]
$(2\pi_g)^3(3\sigma_g^+)$	$(2\pi)^3(4\sigma^+)$	$(1\pi_g)^3(3\sigma_g^+)$	$^1\Pi_g$	Π_g	−1[c]
			$^3\Pi_g$	Π_g	−1[c]
				Σ_g^+	
				Σ_g^-	
				Δ_g	
$(\delta_g)^3(3\sigma_g^+)$	$(\delta)^3(4\sigma^+)$	$(\delta_g)^3(3\sigma_g^+)$	$^1\Delta_g$	Δ_g	
			$^3\Delta_g$	Δ_g	
				Φ_g	
				Π_g	+2[c]
		d → p_π or MLCT Transitions[d]			
$(2\sigma_g^+)(2\pi_u)$	$(3\sigma^+)(3\pi)$	$(2\sigma_g^+)(1\pi_u)$	$a^1\Pi_u$	Π_u	+1
			$a^3\Pi_u$	Π_u	+1
				Σ_u^+	
				(Σ_u^-)	
				(Δ_u)	
$(2\pi_g)^3(2\pi_u)$	$(2\pi)^3(3\pi)$	$(1\pi_g)^3(1\pi_u)$	$^1\Sigma_u^+$	Σ_u^+	
			$^3\Sigma_u^+$	(Σ_u^-)	
				Π_u	+2
			$^1\Sigma_u^-$	(Σ_u^-)	
			$^3\Sigma_u^-$	Σ_u^+	
				Π_u	+2
			$^1\Delta_u$	(Δ_u)	
			$^3\Delta_u$	(Δ_u)	
				(Φ_u)	
				Π_u	0
$(\delta_g)^3(2\pi_u)$	$(\delta)^3(3\pi)$	$(\delta_g)^3(1\pi_u)$	$^1\Phi_u$	(Φ_u)	
			$^3\Phi_u$	(Φ_u)	
				(Γ_u)	
				(Δ_u)	
			b $^1\Pi_u$	Π_u	+1
			b $^3\Pi_u$	Π_u	+1
				Σ_u^+	
				(Σ_u^-)	
				(Δ_u)	
		LMCT Transitions[d,e]			
$(1\pi_u)^3(3\sigma_g^+)$	$(1\pi)^3(4\sigma^+)$		$^1\Pi_u$	Π_u	+1
			$^3\Pi_u$	Π_u	+1
				Σ_u^+	
				(Σ_u^-)	
				(Δ_u)	
$(1\sigma_u^+)(3\sigma_g^+)$	$(2\sigma^+)(4\sigma^+)$	$(1\sigma_u^+)(3\sigma_g^+)$	$^1\Sigma_u^+$	Σ_u^+	
	$(1\sigma^+)(4\sigma^+)$		$^3\Sigma_u^+$	(Σ_u^-)	
				Π_u	+2
$(1\pi_g)^3(2\pi_u)$	$(1\pi)^3(3\pi)$		$^1\Sigma_u^+$	Σ_u^+	
			$^3\Sigma_u^+$	(Σ_u^-)	
				Π_u	+2
			$^1\Sigma_u^-$	(Σ_u^-)	
			$^3\Sigma_u^-$	Σ_u^+	
				Π_u	+2
			$^1\Delta_u$	(Δ_u)	
			$^3\Delta_u$	(Δ_u)	
				(Φ_u)	
				Π_u	0
$(1\sigma_g^+)(2\pi_u)$	$(2\sigma^+)(3\sigma)$	$(1\sigma_g^+)(1\pi_u)$	$^1\Pi_u$	Π_u	+1
	$(1\sigma^+)(3\pi)$		$^3\Pi_u$	Π_u	+1
				Σ_u^+	
				(Σ_u^-)	
				(Δ_u)	

[a] Notation as in Figure 5; filled orbitals omitted. Ground states: $...(2\pi_g)^4(\delta_g)^4(2\sigma_g^+)^2$, $^1\Sigma_g^+$; $...(2\pi)^4(\delta)^4(3\sigma^+)^2$, $^1\Sigma^+$; $...(1\pi_g)^4(\delta_g)^4(2\sigma_g^+)^2$, $^1\Sigma_g^+$. [b] For $C_{\infty v}$ states parity subscripts are dropped. [c] Herzberg–Teller approximation: $h = \sigma_u^+$, $N = \Pi_u$, excited-state mixing only. [d] Dipole-forbidden spin–orbit states in parentheses. [e] Parity-forbidden states not included.

weak d → s transitions of spin-forbidden origin would be expected at lower energy than those associated with the spin-allowed states.

In contrast to the d → s assignments for $AuCl_2^-$ and $AuBr_2^-$, the two weak bands, bands I and II, for AuI_2^- behave differently. Earlier low-temperature measurements[3] showed that their intensity does not decrease on cooling to 26 K. In addition some weak, temperature-dependent absorption features were also resolved at 26 K in the region of bands I and II and were ascribed to the d → s transitions analogous to those of $AuCl_2^-$ and $AuBr_2^-$. Bands I and II for AuI_2^- were therefore assigned as allowed, but weak, LMCT transitions to predominantly spin-forbidden states. The MCD in the region of bands I and II for AuI_2^-, which was not

possible to study in our earlier study, also shows a different pattern compared to that of $AuCl_2^-$ and $AuBr_2^-$. A positive A term is observed for band I of AuI_2^-, and even though the MCD for band II overlaps with the much stronger MCD for band III, the minimum is observed at lower energy (3.31 μm^{-1}) than the absorption maximum (3.46 μm^{-1}), suggesting a positive A term for band II also. The value of $\bar{A}_1/\bar{D}_0$ for band I is probably not very precise in view of the weak vibronic band resolved at low temperature between bands I and II, but the value is definitely positive in contrast to the negative values found for band I for $AuCl_2^-$ and $AuBr_2^-$. Therefore, we reaffirm the assignment of band I of AuI_2^- to a transition to a LMCT Π_u state. Possible candidates are $\Pi_u(^3\Sigma_u^-)$ or $\Pi_u(^3\Sigma_u^+)$ from $(1\pi_g)^3(2\pi_u)$ or $\Pi_u(^3\Pi_u)$ from $(1\pi_u)^3(3\sigma_g^+)$. Our earlier interpretation[3] placed the states of the $(1\pi_g)^3(2\pi_u)$ configuration slightly lower than those of $(1\pi_u)^3(3\sigma_g^+)$, but it must be admitted that the results to date cannot distinguish between the states of the two configurations.

The higher energy, more intense bands II and III for $AuCl_2^-$ were previously assigned as d → p transitions to Π_u states.[3] The new MCD spectra are in good agreement with the earlier MCD results and show a well-defined positive A term for band II but only the lower energy half of a positive A term for band III. The assignment for band II was given as a Π_u state of the $(2\sigma_g^+)(2\pi_u)$ configuration. However, the observed $\bar{A}_1/\bar{D}_0$ value (+1.8) is too large for the states derived simply from $a^1\Pi_u$, $b^1\Pi_u$, $a^3\Pi_u$, or $b^3\Pi_u$ (+1 predicted, Table III). The larger value of $\bar{A}_1/\bar{D}_0$ may indicate the Π_u state has a large contribution from $^3\Sigma_u^+$ or $^3\Sigma_u^-$ of the $(2\pi_g)^3(2\pi_u)$ configuration, but the relatively high intensity of band II indicates a significant $a^1\Pi_u$ or $b^1\Pi_u$ component must be present also. It is important to note that each of the Π_u states of the d → p excited configurations of Table III will mix due to the strong spin–orbit coupling of the Au 5d and 6p orbitals. An individual $\Pi_u(i)$ spin–orbit state will have the form in eq 3, where a_i–g_i are

$$|\Pi_u(i)\rangle = a_i|a^1\Pi_u\rangle + b_i|a^3\Pi_u\rangle + c_i|^3\Sigma_u^+\rangle + d_i|^3\Delta_u\rangle + e_i|^3\Sigma_u^-\rangle + f_i|b^3\Pi_u\rangle + g_i|b^1\Pi_u\rangle \quad (3)$$

the mixing coefficients among the singlet and triplet zero-order states in the absence of the spin–orbit interaction. When several terms of eq 3 contribute nearly equally, it becomes difficult to identify the spin–orbit state with a specific singlet or triplet state. The large $\bar{A}_1/\bar{D}_0$ value observed for band II is taken to indicate extensive spin–orbit mixing between the Π_u states of $(2\sigma_g^+)(2\pi_u)$ and $(2\pi_g)^3(2\pi_u)$ rather than a Π_u state of $(2\sigma_g^+)(2\pi_u)$ alone. Finally, the assignment of band III for $AuCl_2^-$ as another d → p transition to a Π_u state seems reasonable since the MCD appears to cross the zero point near the energy of the absorption maximum. A total of seven Π_u states of the type in eq 3 are expected from the d → p excited configurations, the remaining five are assumed to lie at higher energy or to have transitions to them too weak to be observed.

The higher energy intense bands for $AuBr_2^-$ and AuI_2^- have been assigned to a combination of d → p and LMCT transitions.[3] When compared to the two intense bands of $AuCl_2^-$ (band II at 4.78 μm^{-1} and band III at 5.14 μm^{-1}), the d → p bands III and IV for $AuBr_2^-$ at 4.71 and 4.99 μm^{-1} and bands V and VI for AuI_2^- at 4.59 and 4.92 μm^{-1} show only a small spectral shift as Cl^- is replaced by Br^- and I^-. It was argued that the metal-based d → p type transition should not have a high sensitivity to the nature of the ligand. In contrast, bands III and IV for AuI_2^- at 4.03 and 4.32 μm^{-1}, together with the weak bands I and II discussed above, were assigned as LMCT. Evidence was presented for corresponding LMCT transitions for $AuBr_2^-$ for the shoulder band II near 4.50 μm^{-1} and a band resolved at 26 K at 4.86 μm^{-1}. Analogous bands for $AuCl_2^-$ were assumed to be >5.0 μm^{-1}. The much greater sensitivity of the LMCT band positions to the nature of the ligand is expected, as is the energy ordering $Cl^- > Br^- > I^-$ for corresponding transitions. The present MCD measurements on the intense bands for $AuBr_2^-$ and AuI_2^- are in good agreement with our earlier results. A detailed interpretation of the AuI_2^- bands, including the effects of I^- spin–orbit coupling, was presented earlier.[3] The red shift of LMCT band systems among the comparatively stationary d → p bands from Cl^- to Br^- to I^- is a noteworthy feature of the AuX_2^- spectra.

$Au(PEt_3)_2^+$ Spectra. The absorption and MCD spectra obtained for $Au(PEt_3)_2^+$ (Figure 4) are remarkably similar to that found earlier[4] for $Au(P(OMe)_3)_2^+$. This similarity in spectra, together with the similarity of ligand donor, argues for an analogous interpretation. Specifically the intense band IV and the shoulder band III at 4.88 and 4.78 μm^{-1}, respectively, for $Au(PEt_3)_2^+$ are exactly analogous to an intense band at 4.92 μm^{-1} and a weaker shoulder at 4.70 μm^{-1} in the absorption spectra of $Au(P(OMe)_3)_2^+$. These two transitions were assigned to the $\Pi_u(a^1\Pi_u)$ $[(2\sigma_g^+)(1\pi_u)]$ and $\Pi_u(b^1\Pi_u)$ $[(\delta_g)^3(1\pi_u)]$ states, respectively, on the basis of some spin–orbit calculations for the related $Au(CN\text{-}Et)_2^+$ and $Au(CN)_2^-$ complexes, which also have very similar spectra.[4] An analogous assignment for bands IV and III for $Au(PEt_3)_2^+$ here is reasonable. The MCD is expected to show positive A terms for transitions to both states, and since the absorption bands are only incompletely resolved, the observed MCD is interpreted as two unresolved positive A terms centered at 4.87 μm^{-1}. The B-term contributions to the MCD from the two close-lying Π_u states were predicted to be small in comparison to those of the A terms,[4] but they may be partly responsible for the unsymmetrical appearance of the A term in the regions of bands IV and III. The weaker bands at lower energy for $Au(PEt_3)_2^+$, bands I and II, together with a third unresolved transition corresponding to the MCD minimum at 4.68 μm^{-1}, are logically assigned to the spin–orbit states of $a^3\Pi_u$ and $b^3\Pi_u$ parentage. Analogous weaker bands and associated MCD features are observed and assigned this way for $Au(P(OMe)_3)_2^+$. These assignments were also supported by the spin–orbit calculations, which placed the $\Sigma_u^+(a^3\Pi_u)$ and $\Pi_u(a^3\Pi_u)$ spin–orbit states lowest in energy and quite close together.[2,4] In addition to the positive A term expected for the $\Pi_u(a^3\Pi_u)$ state, the close-lying Σ_u^+ and Π_u states (within transition bandwidths) were shown to give rise to a substantial pseudo-A term from overlapping B terms of opposite sign. With the $\Sigma_u^+(a^3\Pi_u)$ state slightly lower in energy than the $\Pi_u(a^3\Pi_u)$ state, the B terms predicted a positive pseudo-A term, which reinforces the positive A term of the $\Pi_u(a^3\Pi_u)$ state. The observed MCD for band I of $Au(PEt_3)_2^+$ is identical with the A- and B-term pattern found for $Au(P(OMe)_3)_2^+$ and also that observed for several other Au(I) complexes of π-acceptor ligands[4] and therefore is assigned as the pseudo-A-term and A-term combination for the $\Sigma_u^+(a^3\Pi_u)$ and $\Pi_u(a^3\Pi_u)$ states. Band II for $Au(PEt_3)_2^+$ and the unresolved transition associated with the MCD minimum at 4.68 μm^{-1} are likely due to the transitions to $\Pi_u(b^3\Pi_u)$ and $\Sigma_u^+(b^3\Pi_u)$, respectively. Our earlier spin–orbit calculations placed these states in this energy region, but it must be admitted that the spectral assignments cannot be made unambiguously because of the uncertainty of the term assignment of the MCD feature at 4.68 μm^{-1} without knowledge of the precise location of the unresolved absorption. If this feature is a negative B term, as suggested by our earlier calculation, then the MCD would be consistent with our assignment. Otherwise, the feature may be due to a state from the $(2\pi_g)^3(1\pi_u)$ configuration assumed to be at higher energy. The high-energy bands for $Au(PEt_3)_2^+$, bands V and VI, are probably also associated with states of this higher energy configuration, but detailed assignments are not possible because of poor absorption resolution from a rising intense absorption in this region and incomplete MCD data due to instrumental spectral limitations.

$AuX(PR_3)$ Spectra. When compared to the spectra of the $D_{\infty h}$ ions, the absorption and MCD spectra of the $AuX(PR_3)$ complexes exhibit a number of definite similarities, which provide some help in the interpretation. Thus, the spectra for $AuCl(PR_3)$ and $AuBr(PEt_3)$ show a very similar pattern, which is quite similar to that for $Au(PEt_3)_2^+$. This observation points to the conclusion that the transitions in these complexes are predominantly MLCT and that the LUMO is 3π (Figure 5). The lowest energy bands for the chloro– and bromo–phosphine complexes are blue shifted by 0.26–0.30 μm^{-1} compared to band I of $Au(PEt_3)_2^+$; a similar blue shift is observed for the most intense bands (band IV or V for $AuCl(PMe_3)$ or $AuCl(PEt_3)$ and band III for $AuBr(PEt_3)$ compared to band IV of $Au(PEt_3)_2$). This small blue shift on

replacement of a PEt_3 ligand by Cl^- or Br^- can be explained by assuming a reduced P-donor π involvement in the 3π LUMO compared to the $1\pi_u$ orbital of $Au(PEt_3)_2^+$, but it should be noted that changes in electronic repulsions between the cationic and the neutral complexes could also cause small shifts in corresponding excited states. It is interesting that there are also small differences in the spectra between $AuCl(PMe_3)$ and $AuCl(PEt_3)$; the bands of the PEt_3 complex are systematically shifted by 0.03–0.05 μm^{-1} to lower energy. This systematic shift is consistent with a small charge reduction on the Au atom due to a greater inductive σ-donor ability of the PEt_3 ligand compared to PMe_3. A similar effect is observed in the Mössbauer and ^{31}P NMR spectra for the related $AuCl(PR_2Ph)$, R = Me and Et, complexes.[12]

Unlike the MLCT pattern observed for $AuCl(PR_3)$ and $AuBr(PEt_3)$, the absorption and MCD spectra for $AuI(PEt_3)$ resemble the pattern of intense bands exhibited by AuI_2^-, especially the prominent positive A term for band II of $AuI(PEt_3)$ compared with the positive A term for band IV of AuI_2^-. This observation suggests that, as for AuI_2^-, both MLCT and LMCT transitions are present in the spectra of $AuI(PEt_3)$. The lowest energy LMCT configuration is likely $(1\pi)^3(4\sigma^+)$, which gives rise to a $\Pi(^1\Pi)$ excited state for band II of $AuI(PEt_3)$—analogous to the $\Pi_u(^1\Pi_u)$ state of $(1\pi_u)^3(3\sigma_g^+)$ assigned[3] for band IV of AuI_2^-. The slightly lower transition energy for the former (4.20 μm^{-1}) compared to that for the latter (4.32 μm^{-1}) may be rationalized in terms of more stable metal orbitals and lower repulsions in the neutral complex compared to the anion. With this interpretation of band II of $AuI(PEt_3)$ the assignment of band I as due to unresolved transitions to the $\Pi(^3\Pi)$ and $\Sigma^+(^3\Pi)$ states of $(1\pi)^3(4\sigma^+)$ follows naturally. Band III of $AuI(PEt_3)$ at 4.69 μm^{-1} appears analogous to band V of AuI_2^- at 4.59 μm^{-1}, which was assigned as the lowest allowed d $\rightarrow$ p transition to a Π_u state of $(2\sigma_g^+)(2\pi_u)$. The transition for $AuI(PEt_3)$ would be expected to have MLCT character, but the energy difference between the two cases is quite small. This small difference would argue for a relatively minor role for the P-donor π orbitals in the 3π orbital of the $C_{\infty v}$ complex. The slightly lower transition energy for AuI_2^- is probably reflective of less stable Au 5d orbitals due to charge donation from the more reducing I^- ligand, but the difference is small.

When the $AuX(PR_3)$ spectra are compared with that for the AuX_2^- complexes, one notable difference is the absence of the weak vibronic d $\rightarrow$ s bands. The low-energy side of band I for each complex was searched carefully without a suggestion of the weak transitions. This observation can be interpreted as indicating a blue shift of the d $\rightarrow$ s transitions in the $AuX(PR_3)$ complexes. Such a shift might be anticipated since PR_3 is a stronger σ-donor ligand than X^-. Strong σ donation to Au(I) would cause significant antibonding destabilization of the 6s orbital ($4\sigma^+$ in Figure 5), leading to the observed blue shift of d $\rightarrow$ s transitions.

Electronic Structure Conclusions. The observation of the several different types of transitions among the Au(I) complexes studied here indicates that relative orbital energies of the HOMO's and LUMO's are sensitive to ligand type. For example, the HOMO's for $AuCl_2^-$ are 5d Au orbitals and the LUMO's are primarily 6s and 6p on Au. When Cl^- is replaced successively by PR_3 in $AuCl(PR_3)$ and then $Au(PEt_3)_2^+$, the LUMO becomes the P-donor π–Au 6p π combination and the Au 6s orbital is destabilized by carrying a greater σ-bonding interaction. As Cl^- is replaced by Br^- and then I^-, the occupied halide orbitals become less stable and have nearly the same energy as the Au 5d orbital, and when I^- is present, the HOMO shifts from Au 5d to the filled π orbitals of I^-. Because of this sensitivity of the HOMO and LUMO orbitals to ligand type, it is difficult to ascertain the detailed ordering of the Au 5d orbitals in all cases. For the complexes studied here only a limited number of the possible excited states for each transition type could be located. This deficiency prevents firm, unambiguous conclusions, but a few remarks may be worthwhile. While we must admit some ignorance as to the location of all associated states and the exact magnitudes of electronic repulsions (assumed here to be small), the probable ordering of the Au 5d orbitals for the AuX_2^- complexes is $2\sigma_g^+ \gtrsim 2\pi_g > \delta_g$, consistent with the π-donor character of the X^- ligands[3] (the δ_g orbital is nonbonding). The large value of $\bar{A}_1/\bar{D}_0$ for the lowest energy intense band of $AuCl_2^-$ may be rationalized by assuming a Π_u state resulting from extensive mixing between the Π_u states of configurations involving the $2\sigma_g^+$ and the $2\pi_g$ orbitals. This assumption supports the contention that $2\sigma_g^+$ and $2\pi_g$ are the highest Au 5d levels and lie close in energy. The ordering for the Au 5d orbitals for $Au(PEt_3)_2^+$, on the other hand, is likely $2\sigma_g^+ \approx \delta_g > 1\pi_g$, which is consistent with some 5d $\rightarrow$ P-donor π bonding. The near-degeneracy of the $\Pi_u(a^1\Pi_u)$ and $\Pi_u(b^1\Pi_u)$ states reflects the close similarity in energy of the $2\sigma_g^+$ and δ_g orbitals. The $AuX(PR_3)$ complexes then are expected to have only a very small splitting of the Au 5d orbitals, but there is insufficient data to be precise.

In summary, the general spectroscopic behavior of the Au(I) complexes studied in this and in earlier reports[2,4] can best be explained by assuming a minimal involvement of the Au 5d orbitals in bonding and therefore only a small energy splitting. The systematic spectral shifts as a function of ligand can be rationalized from a consideration of relative orbital stability as a function of ligand charge donation to the Au 6s and $6p_z$ orbitals. This conclusion is also supported by recent calculations that show considerable ligand to metal charge delocalization from the halide ligands into 6s and $6p_z$ orbitals in the AuX_2^- ions.[5]

(12) Al-Saady, A. K. H.; McAuliffe, C. A.; Moss, K.; Parish, R. V.; Fields, R. *J. Chem. Soc., Dalton Trans.* **1984**, 491.